Experimental investigation of nonlinear flow for single rock fractures

S J Zhang[1], X Z Dong[1], B H Wu[1] and C L Wang[2, 3]

1 Zhejiang Institute of Hydrogeology and Engineering Geology, Zhengjiang Ningbo, China
2 School of Civil Engineering, Chongqing University, Chongqing, China
3 Key Laboratory of Geotechnical Engineering Stability Control and Health Monitoring of Hunan Province, Hunan University of Science and Technology, Xiangtan, Hunan, China
E-mail: 370567882@qq.com

Abstract. The hydraulic behavior of rocks is significantly controlled by fracture geometries, such as aperture, contact areas, roughness, interconnections, and so on. However, these characteristics are strongly influenced by the confining pressure conditions. This paper experimentally investigated the nonlinear flow behaviors through single rock fractures subjected to a wide range confining pressures. A series of transient pulse tests were conducted on three fractured limestone samples by MTS815 Rock Mechanics Test System. The experimental results show that the pulse decay curves diverge from the classical exponential model due to nonlinearity, thus an empirical relationship between differential pressure and time is developed with consideration of nonlinearity. Subsequently, the nonlinear flow coefficient and permeability were calculated based on the Forchheimer equation. The calculated results show that nonlinear flow coefficient increases with confining pressure, and rougher fracture surface helps to stronger nonlinearity. As the confining pressure increases, the permeability first experiences a dramatic decrease and then behaviors a much slow-down drop. The critical confining pressure for climb-rush shifts increases with the fracture rouhghness.

1. Introduction

Fluid flow in fractured rock masses exists in numerous industrial and scientific fields, such as excavation of rock caverns[1], oil or natural gas exploration[2], [3], contaminant pollution control, hazardous wastes isolation[4], [5] and grouting activities [6]-[8]. Microcracking induced by repository excavation and hydraulic pressure will significantly enhance the permeability in the disturbed zone of the surrounding rocks [5], raise the risk of radionuclide migration across the natural barrier system, and hence cause environment pollution. Therefore, the knowledge of fluid flow behavior through fractured rocks is crucial to pollution prevention and proper management of natural resources.

Fluid flow through single rock fractures obeys the basic law of fluid dynamics [9]. It can be well described by Navier-Stokes (NS) equations. However, how to solve the NS equations in rough-walled fracture is a challenging task due to the inertia term of the N-S equations and irregular geometry of rock fracture [10]. To circumvent the problem, early studies assume that laminar flow occurs between two parallel plates and yields the well-known cubic law. However, the real fracture surfaces are rough which makes the evolution of fluid flow deviate from the cubic law. More importantly, deviation from linear Darcy's law (i.e. nonlinear flow) may occur in rock fractures [11], [12]. The mechanisms that trigger nonlinearity in rough-walled fracture have been extensively studied, including fracture

geometries [13], [14], solid-water interaction [15], turbulence, and localized eddy formation [16]. Previous studies suggest that flow through rock fractures generally occurs in the linear and transitional regimes in real hydrogeological environment [11], [13], [17]. Therefore, this paper mainly focuses on the nonlinear flow as a result of heterogeneity of fracture geometries at low Reynolds number.

Steady-flow method and transient-pressure method are the two major techniques for fluid flow tests. The steady-flow method usually consists of imposing a constant pressure gradient to a sample and measuring the flow rate. This method can easily obtain the relation of pressure gradient and flow rate, so it has been widely applied to investigate the nonlinear flow behavior [9], [11], [18]. However, for low permeability geo-materials, steady-flow method requires a relatively long test time to enhance the measurement accuracy. The transient-pressure method is based on the analysis of the differential pressure between upstream and downstream circuits within a sample, which is appropriate for low permeability geo-materials, and has accurate results better than 5% of results from steady-flow method [19], [20]. Although pulse transient technique has been applied for permeability measurement in rocks fractures [18], [15], few attempts have been made at measuring the nonlinear flow behavior due to the non-steady flow state of the method. In this paper, we develop a new methodology to analyse nonlinear flow for pulse transient tests by calculating instantaneous velocity.

In this paper, the water flow behavior through rough-walled fractures is investigated experimentally using transient pulse method. The observed differential pressure data is analysed to estimate the nonlinearity. Then, the nonlinear flow coefficient and permeability are calculated using Forchheimer law. The relationship between non-Darcy coefficient and confining pressure is explored, and the regression analysis of experimental data is conducted.

2. Experimental methodology

Three limestone samples (M01, M02 and M03) for flow tests were cored from the Mei Tan-ba coal mine in Hunan Province (China). Samples were cut into cylinders by stone processing machine with dimensions of 50 mm in diameter and 100 mm in length. The mechanical properties of samples are shown in Table 1. An artificial fracture was created along the core axis in the uniaxial compressive apparatus using Brazilian technique as illustrated in Figure 1. Before being pre-fractured, the sample was circumferentially applied with glue and covered with thermo-shrinking plastic pipe to avoid sample shattering. Note that the artificial fractures were generated at a loading rate of 50N/s for sample M01, 100N/s for M02 and 200N/s for M03 respectively to achieve different roughness. Visual inspection showed that initial profile of sample M01 is smoother than for samples M02 and M03. And the fracture roughness of samples is measured by a dimensional parameter *JRC* using the method from [21], which gives *JRC* values of 8.96, 13.3 and 14.6 of sample M01-M03, respectively.

$$JRC = 32.2 + 32.471 \lg Z_2 \tag{1}$$

$$Z_2 = \sqrt{\frac{1}{L}\sum_{i=1}^{n}\frac{\left(y_{i+1}-y_i\right)^2}{\left(x_{i+1}-x_i\right)}} \tag{2}$$

where *JRC* is rock roughness, L is the length of sample, x_i is the ith measurement step, y_i is the ith discrete point of y-axis, n is the number of cross-section of discrete points.

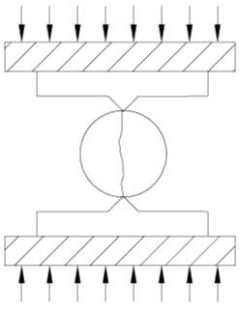

Figure 1 Splitting test

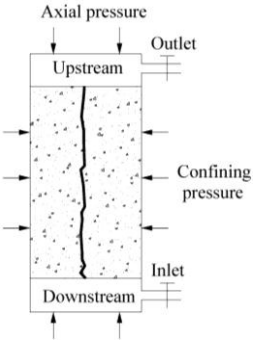

Figure 2 Sketch of transient pulse test

Table 1. Mechanical property of samples

Density (g/cm3)	Porosity	Poisson's ratio	Elastic modulus (GPa)	Uniaxial compressive strength (MPa)
2.61	8.5%	0.23	20.1	44.8

2.1. Experimental setup and procedure

The permeability test was carried out by MTS815 Rock Mechanics Test System using transient pulse method. The system is mainly composed of four units including triaxial cell, loading unit, pressure monitoring unit, water supply unit. The experimental setup has the maximum loading capacity of 4600 kN, and the maximum confining pressure and pore water pressure both are 140 MPa.

Figure 2 shows the sketch of transient pulse test, and the test procedures are summarized as follows:

(1) Produce fractured samples as introduced earlier, saturate the prepared samples with water for 24h.

(2) Install the sample into the triaxial cell, apply the axial and confining pressure to predetermined value at a rate of 0.5MPa/min.

(3) Apply the initial water pressure of 0.2 MPa to the upstream and downstream reservoirs.

(4) Increase the pressure of upstream reservoirs by 2 MPa to form a differential pressure, monitor the change of differential pressure with time until equilibrium is attained.

(5) Increase confining pressure to the next predetermined value and repeat the process (4) to conduct next flow test. For these flow tests, confining pressures were increased from 8 MPa to 20 MPa in gradual levels of 2 MPa.

3. Experimental methodology

3.1. Analysis of pulse decay curves

The evolution of all measured differential pressure is analysed for three samples successively, with the main results being exemplified by sample M01. Simplified analytical methods approach the differential pressure with an exponential formulation [19],

$$\Delta P(t) = \Delta P_0 \exp(-ct) \tag{3}$$

where c is a constant depending on the experimental arrangement. Theoretically, parameter c is a function of reservoir volumes, fluid compressibility, sample accumulation coefficient and external factors such as stress conditions [19]. Figure 3 shows the pulse decay curves of sample M01 at varying confining pressures. The figure demonstrates that the pulse decay curves diverge from the classical exponential model (Equation (3)), especially under high confining pressure. Similar experimental results have also been reported in laboratory tests [15]. The most reasonable explanation is that a nonlinear flow behavior occurs in real rock fractures for their rough walls and variable surface [9]. Previous literatures manifest that the presence of asperities and obstructions or sharp changes in fracture profile will change flow velocity or direction along the flow path, causing inertial losses which make flow regimes deviate from linearity. Meanwhile, the fracture closure and contact areas increase with the confining pressure, which lead to more inertial losses and hence cause nonlinearity.

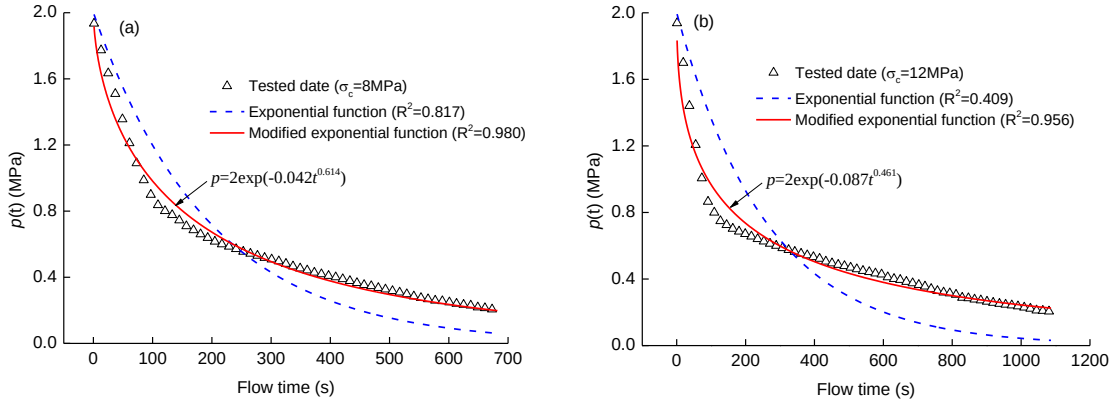

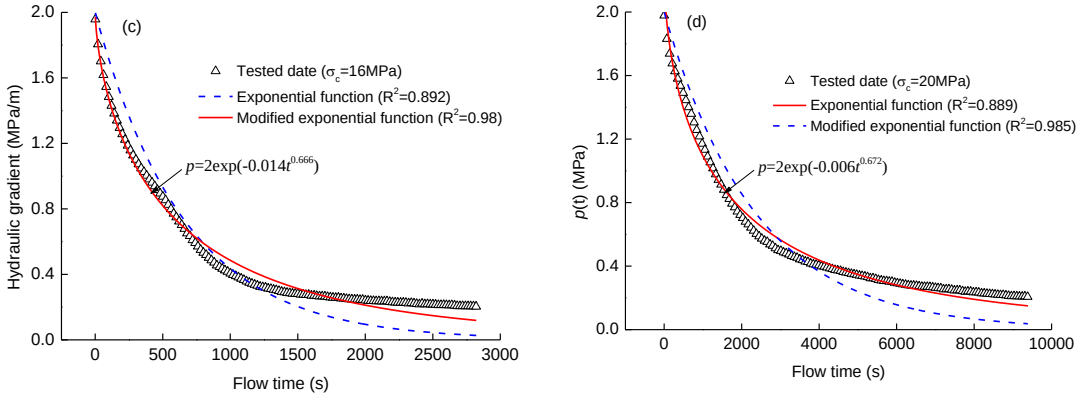

Figure 3 Differential pressure-flow time data and fitting curves for sample M01 at a confining pressure of (a) 8 MPa; (b) 12 MPa; (c) 16 MPa and (d) 20 MPa

Ignoring the volume change of the reservoirs due to the applied water pressure, the variation of the water mass (m_w) in the upstream reservoir can be expressed as [15], [22]

$$\frac{dm_w}{dt}=V_u\frac{d\rho}{dt}=-\rho Av \tag{4}$$

where A is the sectional area of sample; V_u is the volume of reservoir; ρ is the fluid density; and v is the flow velocity through the fracture. The compressibility of water C_f can be expressed as [22]

$$\frac{1}{C_f}=\rho\frac{dp_1(t)}{d\rho} \tag{5}$$

Combination of Equations (4) and (5) gives

$$\frac{dp_1(t)}{dt}=-\frac{Av}{C_fV_u} \tag{6}$$

Similarly, we obtain the following equation for the downstream reservoir:

$$\frac{dp_2(t)}{dt}=\frac{Av}{C_fV_d} \tag{7}$$

Combination of Equations (6) and (7) yields

$$\frac{dp(t)}{dt}=\frac{dp_1(t)-dp_2(t)}{dt}=-\frac{Av}{C_f}\left(\frac{1}{V_u}+\frac{1}{V_d}\right) \tag{8}$$

Or

$$v=-\frac{C_f}{A\left(\frac{1}{V_u}+\frac{1}{V_d}\right)}\frac{dp(t)}{dt} \tag{9}$$

The hydraulic gradient j at time t can be simply calculated using the experimental pulse decay data, i.e.

$$j=\frac{p(t)}{L}=\frac{p_1(t)-p_2(t)}{L} \tag{10}$$

It can be seen from Equations (9) and (10) that the experimental pulse decay data can be used as a criterion of linear or nonlinear flow. If the pulse decay data follows the classical exponential formulation (Equation (3)), the relationship between the velocity and pressure gradient is linear, which means linear flow occurs. Otherwise, nonlinear flow occurs. Obviously, in this paper, the relationship between flow velocity and hydraulic gradient doesn't meet the Darcy's law, indicating that a nonlinear flow behavior occurs. The nonlinear flow characteristics will be further discussed in detail later.

To have a best-fit regression analyses of the experimental pulse decay data, p(t), a modified exponential equation is proposed, i.e.

$$p(t)=p_0\exp\left(-ct^n\right) \tag{11}$$

where *n* is a fitting parameter depending on the nonlinearity. By selecting an appropriate value of *n*, a high correlation coefficient can be obtained for the fitting equation. Note that the general exponential formulation (Equation (11)) can reduce to traditional formulation (Equation (3)) for value of *n*=1 when the flow occurs in the linear regime. The experimental data are fitted using this modified and more general exponential formulation and the fitting curves are shown in the Figure 3. It can be clearly seen that the generalized model provides a better fit than the exponential model given by Equation (3).

3.2. Analysis of non-Darcy flow

Previous studies [11], [18] indicate that Forchheimer law has proved to fit the flow in fractured rocks well. For a one-dimensional non-Darcy flow, the relationship between pressure and flow velocity can be expressed as [23]

$$\rho c_a \frac{dv}{dt} = -j - \frac{\mu}{k} v + \rho \beta v^2 \tag{12}$$

where c_a is acceleration factor, k is permeability; μ is kinematic viscosity of the fluid. The flow velocity and $\eta = \frac{dv}{dt}$ can be obtained with Equation (9). The differential pressure $\left(p_1 - p_2\right)_{t=i} \left(i = 1,2 \cdots n\right)$ were measured every 1.0 s. Therefore, the following equitation is satisfied

$$\rho c_a \eta_i = -j_i - \frac{\mu}{k} v_i + \rho \beta v_i^{\,2} \left(i = 1,2 \cdots n-2\right) \tag{13}$$

Establishing a fonctionelle $\prod$

$$\prod = \sum_{i=2}^{N-2} \left(\rho \beta V_i^2 - \frac{\mu}{k} V_i - \rho c_a \eta_i - \xi_i \right)^2 \tag{14}$$

By solving the fonctionelle $\prod$ on basis of extremum conditions, we can obtain β and k.

$$\frac{\partial \prod}{\partial(\rho\beta)} = 0; \left(\sum_{i=2}^{N-2} V_i^4 \right) \rho\beta - \left(\sum_{i=2}^{N-2} V_i^3 \right) \frac{\mu}{k} - \left(\sum_{i=2}^{N-2} \eta_i V_i^2 \right) \rho c_a - \left(\sum_{i=2}^{N-2} \xi_i V_i^2 \right) = 0 \tag{15}$$

$$\frac{\partial \prod}{\partial\left(\frac{\mu}{k}\right)} = 0; \left(\sum_{i=2}^{N-2} V_i^3 \right) \rho\beta - \left(\sum_{i=2}^{N-2} V_i^2 \right) \frac{\mu}{k} - \left(\sum_{i=2}^{N-2} \eta_i V_i \right) \rho c_a - \left(\sum_{i=2}^{N-2} \xi_i V_i \right) = 0 \tag{16}$$

$$\frac{\partial \prod}{\partial(\rho c_a)} = 0; \left(\sum_{i=2}^{N-2} V_i^2 \eta_i \right) \rho\beta - \left(\sum_{i=2}^{N-2} V_i \eta_i \right) \frac{\mu}{k} - \left(\sum_{i=2}^{N-2} \eta_i^2 \right) \rho c_a - \left(\sum_{i=2}^{N-2} \xi_i \eta_i \right) = 0 \tag{17}$$

3.2.1 Relation of k and confining pressure.

Figure 4a-c shows the relation of permeability and confining pressure for tested samples. As the confining pressure increases, permeability of three samples first experiences a dramatic decrease and then behaviors a much slow-down drop. This can be integreted that the fracture aperture decreases sharply due to the favourable fracture compressibility, and then decreases at a much slower speed due to fracture closure when the confining pressure is higer than the fracture closure stress. Comparing with Figure 4(a), Figure 4(b) and Figure 4(c), it is found that the sample M03 with the largest *JRC* value shows the minimum permeability, M02 takes the second place, while M01 shows the maximum permeability. This further emphasis the common knowledge that rocks with smoother fracture surfaces have a larger permeability. Note that the drop shift of $k - \delta_c$ curve for three samples are different. In general, the critical confining pressure for drop shift increases with the fracture rouhghness. Specificly, the threshold value of Sample M01<Sample M02<Sample M03. This phenomenon would possibly result from that a rougher fracture needs a larger stress to make the fracture surfaces joint closely. To characterize the relation between permeability and confining pressure for fractured rock, Ma et al. [18] proposed a power function to fit the obserted data.

$$k = a_1 \sigma_c^{\,b_1} \tag{18}$$

where k is the permeability, σ_c is the confining pressure, the coefficient a_1 and b_1 are scaling parameters. As shown in Figure 4a-c, the power function given by Equation (18) fits the experimental data well, supporting the usefulness of the power function.

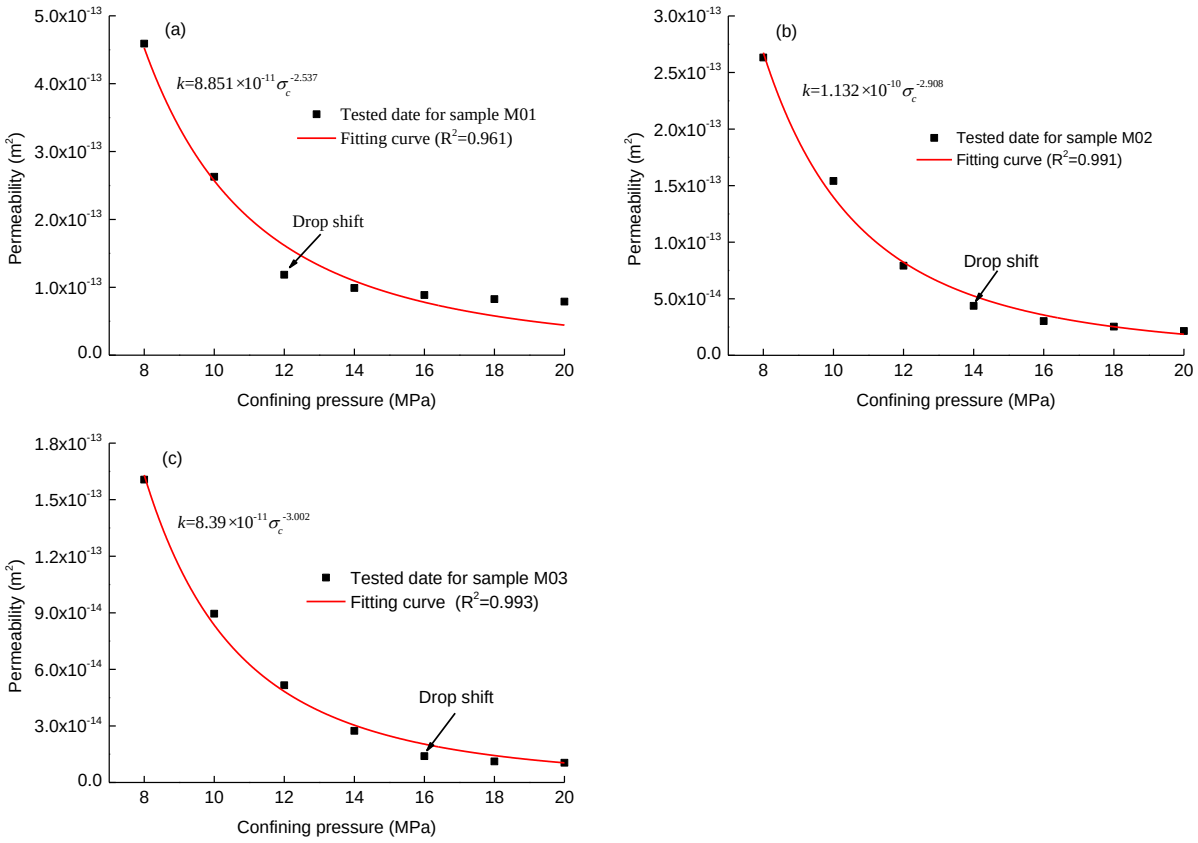

Figure 4 Permeability k-confining pressure curves of sample (a) M01; (b) M02 and (c) M03

3.2.2 Relation of β and confining pressure.

Figure 5 demonstrates that the non-Darcy flow coefficient β increases with confining pressure at a decreasing change rate, indicating that higher confining pressure helps to stronger nonlinearity. The values of non-Darcy flow coefficient β, in decreasing order, are those of test samples M01 (minimum), M02 and M03 (maximum) for a given confining pressure. This can be integrated as a rougher fracture shows a stronger nonlinear flow behavior at the same condition of confining pressure. Such trend is in qualitative agreement with the experimental results from Zhou et al. [11], in which he suggests that a rougher fracture surface usullay induces a more dramatic nonlinear flow behavoir due to solid-water interaction.

Ma et al. [18] introduced a logarithmic function and a polynomial function to analyze the relationship between the non-Darcy coefficient β and confining pressure. Figure 5(a)-(c) shows that the logarithmic function didn't match tested data well. The average value of R^2 of the polynomial function is less than 0.9.

$$\beta = a_2 \ln(\sigma_c) + b_2 \tag{19}$$

where σ_c is confining pressure, a_2 and b_2 are fitting parameters. To have a best-fit analysis of tested data, an empirical formula is proposed in this paper.

$$\beta = a_3 \sigma_c \exp(\lambda \sigma_c) + b_3 \tag{20}$$

where a_3 is the scaling parameters, λ gives the slope, and parameter b_3 gives the intercept. It can be seen that the new function provides a better fit than the logarithmic function. For the new function, the

average value of R^2 is close to unit (over 0.99), while for logarithmic function, the average is less than 0.9, indicating that the performance of new function is better than the logarithmic function.

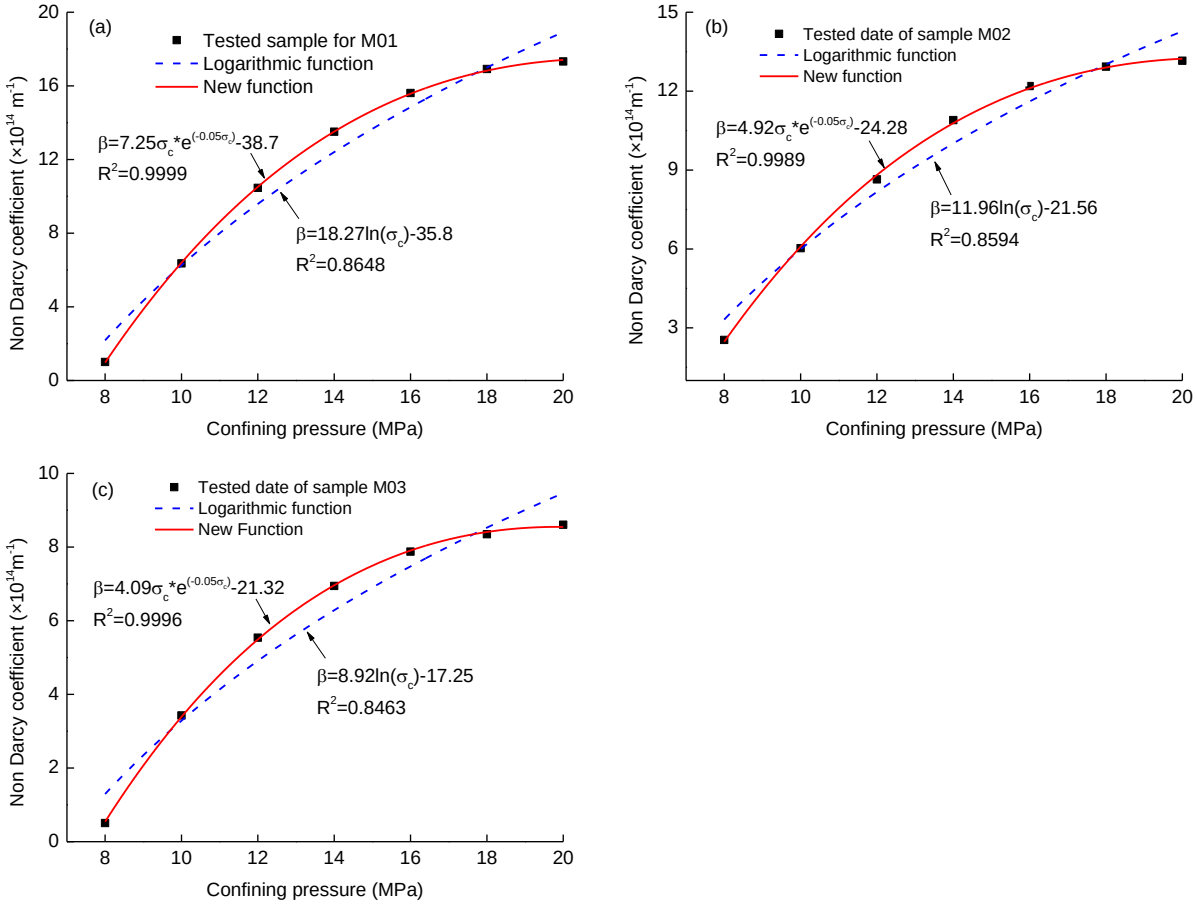

Figure 5 Non-Darcy coefficient -confining pressure curves of sample (a) M01; (b) M02 and (c) M03

4. Conclusions

In this paper, the effects of variable confining pressure on nonlinear flow behaviors of rough-walled fractures are investigated through transient pulse tests, the main conclusions are as follows:

(1) The observed pulse decay data versus time diverges from the classical exponential model due to nonlinear flow behavior, and then a modified exponential relationship is developed with consideration of nonlinearity. Theoretical derivation gives that the experimental pulse decay data can be used as a criterion of nonlinear flow.

(2) The nonlinear flow coefficient β and permeability k were calculated based on the Forchheimer equation. The calculated results show that β increases with confining pressure, and rougher fracture surface helps to stronger nonlinearity.

(3) As the confining pressure increases, the permeability first experiences a dramatic decrease and then behaviors a much slow-down drop. The critical confining pressure for climb-rush shifts increases with the fracture rouhghness.

5. References

[1] Ren F, Ma G, Fu G, et al. Investigation of the permeability anisotropy of 2D fractured rock masses. *Eng Geol*, 2015, 196, 171-182.

[2] Karpyn Z T, Alajmi A, Radaelli F, et al. X-ray CT and hydraulic evidence for a relationship between fracture conductivity and adjacent matrix porosity. *Eng Geol*, 2009, 103(3):139-145.

[3] Wu Y S, Lai B, Miskimins J L, et al. Analysis of multiphase non-Darcy flow in porous media. *Transport Porous Med*, 2011, 88(2): 205-223
[4] Quinn P M, Parker B L and Cherry J A. Using constant head step tests to determine hydraulic apertures in fractured rock. *J Contam Hydrol*, 2011;126(1)85-99.
[5] Chen Y, Hu S, Wei K, Zhou C and Jing L. Experimental characterization and micromechanical modeling of damage-induced permeability variation in Beishan granite. *Int J Rock Mech Min Sci*, 2014, 71:64-76.
[6] Fernandez G and Moon J. Excavation-induced hydraulic conductivity reduction around a tunnel-Part 1: Guideline for estimate of ground water inflow rate. *Tunn Undergr Space Technol*, 2010, 25(5):560-566.
[7] Yang W, Lin B Q, Qu Y A, et al. Stress evolution with time and space during mining of a coal seam. *Int J Rock Mech Min Sci*, 2011, 48(7): 1145-1152.
[8] Shen C M, Lin B Q, Sun C, et al. Analysis of the stress-permeability coupling property in water jet slotting coal and its impact on methane drainage. *J Pet Sci Eng*, 2015, 126:231-241.
[9] Rong G, Yang J, Cheng L, et al. Laboratory investigation of nonlinear flow characteristics in rough fractures during shear process. *J Hydrol*, 2016, 541, 1385-1394.
[10] Brush D J and Thomson N R. Fluid flow in synthetic rough-walled fractures: Navier-Stokes, Stokes, and local cubic law simulations. *Water Resour Res*, 2003, 39 (4), 1-15.
[11] Zhou J Q, Hu S H, Fang S, et al. Nonlinear flow behavior at low Reynolds numbers through rough-walled fractures subjected to normal compressive loading. *Int J Rock Mech Min Sci*, 2015, 80:202-218.
[12] Zou L, Jing L, Cvetkovic V. Roughness decomposition and nonlinear fluid flow in a single rock fracture. *Int J Rock Mech Min Sci*. 2015;75:102-118.
[13] Zimmerman R W, Bodvarsson G S. Hydraulic conductivity of rock fractures. *Transport Porous Med*, 1996, 23(1):1-30.
[14] Tenchine S and Gouze P. Density contrast effects on tracer dispersion in variable aperture fractures. *Adv Water Resour*, 2005 28(3): 273-289
[15] Zhao YL, Zhang LY, Wang W J, et al. Transient pulse test and morphological analysis of single rock fractures. *Int J Rock Mech Min Sci*, 2017, 91:139-154.
[16] Zhang Z, Nemcik J and Ma S. Micro- and macro-behavior of fluid flow through rock fractures: an experimental study. *Hydrogeo J*, 2013, 21(8):1717-1729.
[17] Schrauf T W, Evans D D. Laboratory studies of gas flow through a single natural fracture. *Water Resour Res*, 1986; 22(7)1038-1050.
[18] Ma D, Miao X X, Chen Z Q, et al. Experimental investigation of seepage properties of fractured rocks under different confining pressures. *Rock Mech Rock Eng*, 2013, 46(5):1135-1144.
[19] Davy C A, Skoczylas F, Barnichon J D, et al. Permeability of macro-cracked argillite under confinement: Gas and water testing. *Phys Chem Earth Parts A/B/C*, 2017, 32:667-680.
[20] Wang H L, Xu W Y and Shao J F. Experimental researches on hydro-mechanical properties of altered rock under confining pressures. *Rock Mech Rock Eng*, 2014, 47:485-493.
[21] Tse R and Cruden D M. Estimating joint roughness coefficients. *Int J Rock Mech Min Sci Geomech Abstr*, 1979, 16:303-307.
[22] Dana E and Skoczylas F. Gas relative permeability and pore structure of sandstones. *Int J Rock Mech Min Sci*, 1999, 36(5):613-625.
[23] Ma D, Bai H, Chen Z, et al. Effect of Particle Mixture on Seepage Properties of Crushed Mudstones. Transport Porous Med, 2015, 108(2):257-277.

Acknowledgments
This work was supported by the National Natural Science Foundation of China [grant numbers No.51374257 and No. 50804060] and the Geotechnical Engineering Stability Control and Health Monitoring of Hunan Province Key Laboratory, Hunan University of Science and Technology [grant numbers No. E21619].